Recurrent Rossby wave packets modulate the persistence of dry and wet spells across the globe

S. Mubashshir Ali[1], Olivia Martius[2], and Matthias Röthlisberger[3]

[1]Oeschger Centre for Climate Change Research and Institute of Geography
[2]Mobiliar Lab for Natural Risks, University of Bern
[3]Institute for Atmospheric and Climate Science, ETH Zürich

November 26, 2022

Abstract

Persistent dry and wet spells can arise from stationary weather situations or recurrent flow patterns and result in significant socio-economic impacts. Here, we study the effects of recurrent synoptic-scale transient Rossby wave packets (RRWPs) on the persistence of dry and wet spells using the ERA-Interim reanalysis data. RRWPs significantly alter (decrease and increase) dry and wet spell persistence across the globe. Spatial patterns of statistically significant links between RRWPs and spell durations arise from the superposition of a zonally symmetric component and a wave-like component that is modulated by local factors such as orography and the position relative to major moisture sources. The zonally symmetric component is apparent during the Northern Hemisphere winter and dominates the Southern Hemisphere signal in winter and summer. The wave-like component appears primarily in the Northern Hemisphere, changes its wavenumber with the season and is thus, conceivably related to stationary wave dynamics.

Recurrent Rossby wave packets modulate the persistence of dry and wet spells across the globe

S. Mubashshir Ali[1], Olivia Martius[1,2], Matthias Röthlisberger[3]

[1]Oeschger Centre for Climate Change Research and Institute of Geography, University of Bern, Bern, Switzerland

[2]Mobiliar Lab for Natural Risks, University of Bern, Bern, Switzerland

[3]Institute for Atmospheric and Climate Science, ETH Zürich, Zürich, Switzerland

Corresponding author: S. Mubashshir Ali (mubashshir.ali@giub.unibe.ch)

Key Points

- Recurrent Rossby wave packets significantly alter (lengthen or shorten) the persistence of both wet and dry spells in the extratropics.
- They lengthen or shorten dry (wet) spells through the recurrent formation of ridges (troughs) in the same area.
- Recurrence of transient Rossby waves should be considered as a key dynamical mechanism for fostering persistent surface weather.

Abstract

Persistent dry and wet spells can arise from stationary weather situations or recurrent flow patterns and result in significant socio-economic impacts. Here, we study the effects of recurrent synoptic-scale transient Rossby wave packets (RRWPs) on the persistence of dry and wet spells using the ERA-Interim reanalysis data.

RRWPs significantly alter (decrease and increase) dry and wet spell persistence across the globe. Spatial patterns of statistically significant links between RRWPs and spell durations arise from the superposition of a zonally symmetric component and a wave-like component that is modulated by local factors such as orography and the position relative to major moisture sources. The zonally symmetric component is apparent during the Northern Hemisphere winter and dominates the Southern Hemisphere signal in winter and summer. The wave-like component appears primarily in the Northern Hemisphere, changes its wavenumber with the season and is thus, conceivably related to stationary wave dynamics.

Plain Language Summary

Unchanged weather conditions over a prolonged period (persistent weather) can lead to adverse conditions e.g. in agriculture. Traditionally, such weather conditions are understood to arise from slow-moving (i.e., "stationary") weather systems. In this study, we illustrate an alternative, "non-stationary" atmospheric flow configuration, which can cause such persistent weather by the repeated formation (recurrence) of troughs and ridges in the same areas. The upper-level atmospheric waves, which influence our daily weather, govern this process. We show two example cases, where recurrence leads to persistent dry or wet conditions. By analysing over 35 years of data, we find such wave recurrence to be statistically relevant for persistent dry and wet conditions. For many land areas of both the Northern and the Southern Hemisphere, increased or reduced persistence of dry and wet conditions are related to the recurrent upper-level waves.

1. Introduction

Persistent extreme surface weather events pose a threat to food security, health, livelihood, and property (Kornhuber et al., 2020; Raymond et al., 2020; Rudd et al., 2020; Sivakumar, 2018). Persistent dry conditions can lead to droughts and exacerbate wildfires, whereas persistent wet conditions can lead to flooding. On multi-day to sub-seasonal timescales, persistent conditions may offer windows of high predictability but remain challenging for numerical weather

forecast models (Ferranti et al., 2015; Matsueda & Palmer, 2018). Therefore, fundamental process understanding is essential for improving forecasts of such events (Quandt et al., 2017; Webster et al., 2011), and to reduce uncertainties in the future climate projections.

Persistent dry and wet spells are often related to slow-moving or stationary weather systems. Quasi-stationary blocking anticyclones, (e.g., Rex 1950; Pelly & Hoskins, 2003), are associated with subsidence, and thus, they often exhibit clear-sky conditions in their central and downstream part. Subsidence and increased shortwave radiation at the surface leads to hot and dry surface anomalies (e.g., Li et al. 2020; Pfahl & Wernli, 2012; Quinting et al. 2018; Xu et al., 2020; Zschenderlein et al., 2018; Zschenderlein et al., 2020). The persistence of the blocking anticyclones can then result in long-lasting heatwaves and persistent dry spells (Fang & Lu, 2020; Röthlisberger & Martius, 2019). Persistent wet spells can arise as a result of slow-moving and stalling tropical and extratropical cyclones (e.g; Risser & Wehner, 2017; Rhodes, 2017), persistent monsoon circulation patterns (e.g; Fang et al., 2012), stationary cut-off lows (e.g; Lenggenhager et al., 2019), and as a result of an eastward extension of the jet over the Atlantic (e.g; Blackburn et al., 2008; Schaller et al., 2016). Quasi-stationary waves, in particular those spanning an entire Hemisphere, can also be associated with both persistent dry and wet spells around the globe (Coumou et al., 2014; Kornhuber et al., 2016; Stadtherr et al., 2016; Wolf et al., 2018). However, besides stationary drivers, a number of studies have identified recurrent (rather than stationary) large-scale circulation as a cause for persistent surface weather e.g., (Drouard & Woollings, 2018; Michelangeli et al., 1995).

Recurrence of transient weather systems in the same area on sub-seasonal timescales can be associated with persistent extreme surface temperature conditions. A statistically significant link exists between recurrent Rossby wave packets (RRWPs) and the persistence of winter-cold and summer-hot spells over large areas in the Northern Hemisphere midlatitudes (Röthlisberger et al., 2019). Such RRWPs events are characterized by the repeated passage of transient synoptic-scale Rossby wave packets in the same phase at the same longitudes. Both recurrent ridging or troughing due to RRWPs can result in the persistent hot and cold spells (Röthlisberger et al., 2019). A few notable examples of RRWPs inducing persistent surface weather are the 1994 Central European heat wave (Röthlisberger et al., 2019), the anomalous Northern Hemisphere 2013-14 winter (Davies, 2015; Wolter et al., 2015), and flooding in the Southern Alpine region in fall 1993 (Barton et al., 2016).

Röthlisberger et al. (2019) quantified the climatological effect of RRWPs on the duration of temperature spells in the Northern Hemisphere, while the other studies cited above present case study-based evidence for a link between RRWPs and persistent wet and dry spells. However, a systematic and global evaluation of the effect of RRWPs on the persistence of dry and wet spells is so far missing. The purpose of this paper is twofold: Firstly, we aim to identify regions where the persistence of these spell types is significantly altered by RRWPs. Secondly, we discuss the physical processes linking the upper-level RRWPs to persistent wet and dry surface conditions based on example cases.

2. Data and Method

This study uses ERA-Interim reanalysis data (Dee et al., 2011) on a 1° by 1° spatial resolution for the period 1980-2016. Atmospheric fields are used at 6-hourly temporal resolution. Atmospheric blocking is identified based on upper-level negative potential vorticity (PV) anomalies as in Schwierz et al. (2004), but with a slightly modified algorithm detailed in Rohrer et al., (2018). Daily aggregated precipitation data is used for the identification of dry and wet spells at each grid point. Days with accumulations below (exceeding) 1 mm are classified as dry (wet) days. Spells separated by a one-day gap are merged into one continuous spell. From the resulting sets of dry and wet spells, all spells lasting less than 5 days are discarded, as we motivate our study from an impacts point of view. This procedure results in a set of n_g spells at each grid point g, each with durations $D_{g,1},\ldots,D_{g,ng}$ (Figure S1 and S3).

To assess the effect of RRWPs on dry (wet) spell durations, we have used a Weibull regression model, exactly as in Röthlisberger et al. 2019 and the notation used here is consistent with theirs. They introduced a metric "*R*" as a simple measure of RRWP strength derived from Hovmöller (time-longitude) diagrams of instantaneous meridionally averaged (35°N–65°N) meridional wind at 250 hPa (V250). The R-metric is in essence a time and wavenumber filtered V250 field (refer Röthlisberger et al. 2019 for more details). We have computed this metric also for the Southern Hemisphere from meridionally averaged (35°S–65°S) V250. We used the respective *R* as a covariate in a Weibull regression model fitted to dry and wet spell duration at each grid point in the Northern and the Southern Hemisphere, respectively. Only grid-points having at least 40 spells are considered. Also, grid-points in between 20°N and 20°S are excluded from the analysis. Thus, we assess whether RRWP conditions are associated with a statistically significant increase or decrease of dry and wet spell durations during extended

summer (MJJASO) and extended winter (NDJFMA) in both the Hemispheres. The Weibull model is more complex compared to the standard Gaussian linear model but, it allows us to assess changes in all quantiles of the modelled spell duration distribution per unit increase in each covariate (Supplementary Material in Röthlisberger et al. 2019 introduces Weibull model). Thus, it is possible to assess the effect of RRWPs via the covariate *R* on the entire distribution of spell durations. While the statistical analysis can reveal covariability between *R* and the spell durations, the causality in our statistical arguments is based on the case studies cited above and shown later here and in the Supplementary Material.

The Weibull model is fitted at each grid point and is only briefly introduced here for an arbitrary grid point g. First, a representative value of *R* ($\tilde{R}_{\lambda_g,i}$) is assigned to each spell *i* occurring at this grid point (with longitude λ_g), which quantifies how recurrent the synoptic scale waves are in the 60° longitudinal sector centred on λ_g during the lifetime of a spell *i* (Eq. 1). To calculate the $\tilde{R}_{\lambda_g,i}$, the raw R-metric, which is a function of longitude and time, is longitudinally averaged within the 60-degree longitudinal sector centred on λ_g for each time step. Then, the representative *R* value $\tilde{R}_{\lambda_g,i}$ of spell *i* is computed as the median of these longitudinally averaged *R* values $R_{lon}(\lambda, \mathrm{t})$ during the lifetime of the spell:

$$\tilde{R}_{\lambda_g,i} = \mathrm{median}\{R_{lon}(\lambda, \mathrm{t})\} \quad ; \mathrm{t} = t_{\{\mathrm{g,i}\}}^{\{\mathrm{start}\}}, \ldots., t_{\{\mathrm{g,i}\}}^{\{end\}\}} \qquad \text{(Eq. 1)}$$

The Weibull regression model fitted to the spell durations $D_{g,1}, D_{g,2}, \ldots, D_{g,ng}$ at each grid point g is given by:

$$\ln\left(D_{g,i}\right) = \alpha_{0,g} + \alpha_{1,g}\tilde{R}_{\lambda_g,i} + \sum_{j=2}^{6} \alpha_{j,g} m_j\left(t_{g,i}^{start}\right) + \sigma_g \epsilon_{g,i} \quad ; i = 1, \ldots n \qquad \text{(Eq. 2)}$$

where $\alpha_{0,g}, \alpha_{1,g}, \ldots, \alpha_{6,g}$ are the regression coefficients, $\varepsilon_{g,1}, \ldots, \varepsilon_{g,N\_g}$ are the error terms following the standard extreme minimum value distribution and $\sigma_g > 0$ is a scale parameter. Additionally, $m_2, \ldots, m_6$ are covariates representing dummy variables for each month to account for seasonal variations in spell durations (Röthlisberger et al., 2019). Fitting the model to spell durations at each grid point then results in maps of regression coefficients $\alpha_{1,g}$. The null hypothesis examined here is that RRWPs have no effect on the duration of dry and wet spells, which is rejected at a grid point g if $\alpha_{1,g}$ is significantly different from zero. Two-sided significant departures of $\alpha_{1,g}$ from zero are identified as in Zhang (2016) at a significance level of 0.025 and 0.975.

Hereafter we present the exponentiated regression coefficients $exp(\alpha_1)$ called "acceleration factors" (AF) in survival analysis applications (e.g; Hosmer et al., 2008; Zhang, 2016). The AF $exp(\alpha_{1,g})$ depicts the factor by which all quantiles of the spell duration D_g at a grid point g changes per unit increase in the covariate $\tilde{R}_{\lambda_g,i}$ (Hosmer et al., 2008). Here, we use the AFs to identify statistically significant links between RRWPs and spell durations, and therefore focus on regions where AF is significantly larger or smaller than 1, and not on the AF values themselves. Regions with AF>1 (AF < 1) experience significantly increased (decreased) spell durations with an increasing *R* value, i.e., during RRWP conditions. We tested the sensitivity of our results to changes in the minimum spell duration and the gap duration parameters. We found consistent AF patterns for the minimum spell durations of 4, 5, 6 days with the respective gap duration of 0 and 1 day. However, the gap duration of 1 day improves the null hypothesis, that the spell durations are Weibull distributed, for most of the grid-points. It is tested using the Anderson-Darling test at significance level 0.01.

3 Results

3.1 Examples of persistent wet and dry spells during RRWPs

Two case studies serve to introduce key concepts of this study: a persistent wet episode in Spain, and a persistent dry episode in Brazil. During April-May 1983, persistent wet conditions over the Iberian Peninsula led to a 35-day long wet spell at a grid-point in western Spain (red cross in Figure 1a). The daily precipitation accumulation exceeded the local 90th percentile for 11 days during this spell. While blocking was present over south Greenland during the first 10 days of the spell (Figures 1b and 3a), a series of additional (and clearly distinct) transient wave packets moved across the Atlantic during the subsequent three weeks, which resulted in continuously high R values between 60°W and 30°E (Figure 1b). Recurrent northerly flow conditions over the eastern Atlantic (Figure 1b) resulted in repeated advection of moist air to north-western Spain. Concurrently, positive, and negative precipitation anomalies were also present upstream over the Atlantic basin and downstream in the Mediterranean, all of which were associated with a distinct wave pattern over the Atlantic basin (Figures 1b and 3a), and consequently high R values. Note that no circumglobal wave pattern was present. The negative precipitation anomalies were co-located with the ridges and the positive precipitation anomalies were located downstream of the trough axes (Figure 3a). Interestingly, during this period, atmospheric blocks were also frequent (but not always) over the Gulf of Alaska (Figure 3a).

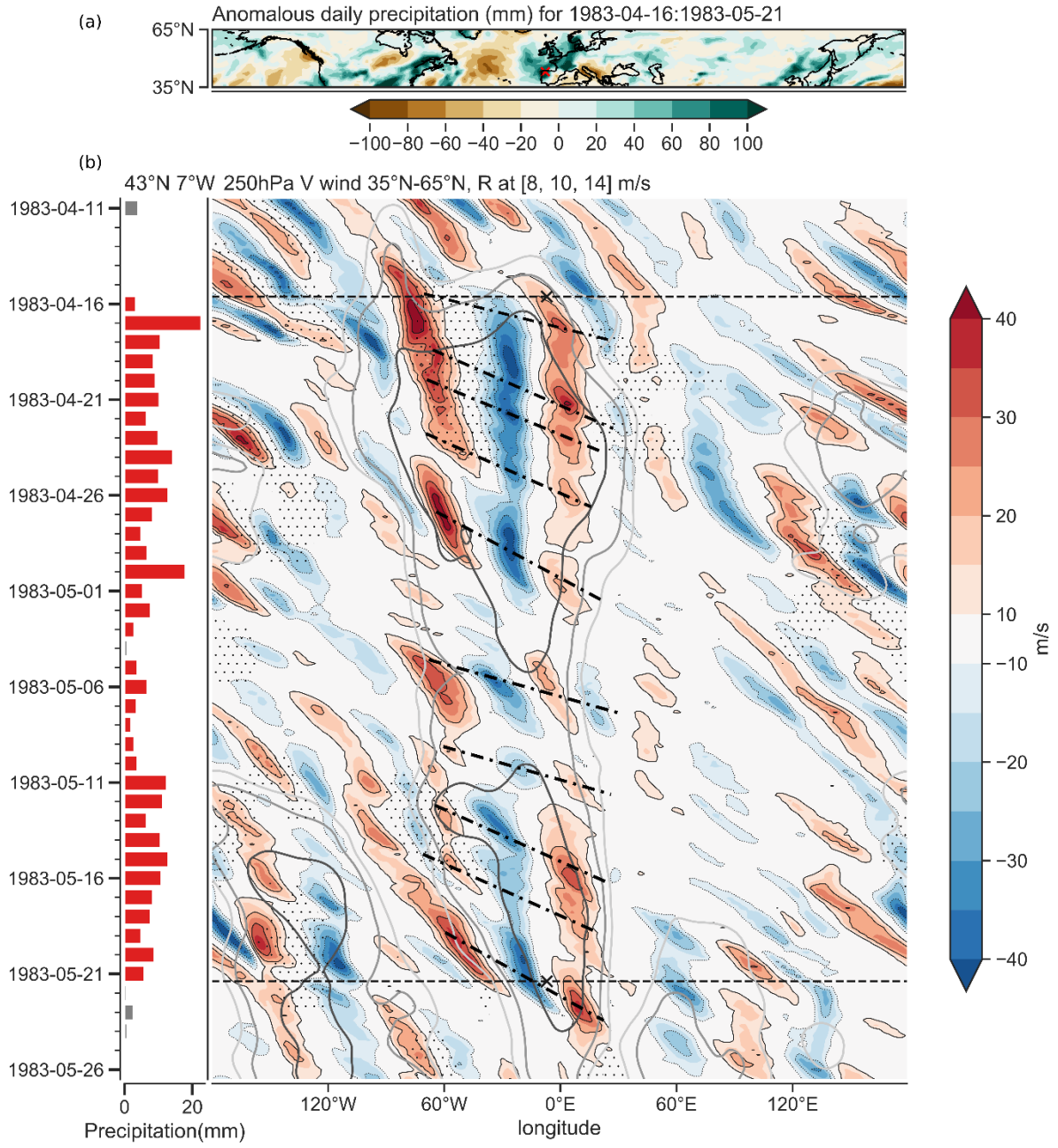

174

175 *Figure 1. An example wet spell during April-May 1983. (a) Anomalous daily precipitation (mm)*
176 *compared to ERA-I climatology (1979-2018) aggregated for the spell duration. (b) Bars show*
177 *aggregated daily precipitation at location 'x' (43°N, 7°W) in (a), red when precipitation is in the spell*
178 *period and above 1 mm threshold, else grey. The Hovmöller diagram in (b) shows 35°N-65°N averaged*
179 *meridional wind at 250 hPa. Black dotted lines in (b) mark the onset and end of the spell at 'x' in (a).*
180 *Grey contours show R values of 8, 10, 14 m/s. Stipplings depicts longitudes at which at least one grid*
181 *point in 20°N-70°N featured an atmospheric block while the dash-dotted lines indicate the approximate*
182 *longitude–time trajectory of the Rossby wave packets (i.e., group propagation).*

In November 1985, recurrent Rossby waves were associated with persistent dry conditions over São Paulo, Brazil, and surroundings (Figure 2). A series of recurrent and non-stationary Rossby wave packets moved across the Southern Pacific in quick succession. It resulted in recurrent ridging over São Paulo (Hovmöller plot in Figure 2b). The wave pattern is also evident in the PV composite for this period (Figure 3b). Interestingly, blocking was not present over the São Paulo region, but two blocks appear over the Indian Ocean (south of Australia), one in the beginning and one towards the end of this period. There is an indication of anticyclonic wave breaking happening upstream of Patagonia in the Southern Pacific Ocean (Figure 3b). Two additional case studies are included in the Supplementary material (Figure S5 and S7). These case studies clearly illustrate that besides blocking, recurrent amplification of troughs and ridges in the same geographical areas can foster persistent dry and wet spells on subseasonal timescales. In the remainder of this study, we, therefore, quantify the effect of RRWPs on the persistence of dry and wet spells climatologically by means of the Weibull regression introduced above.

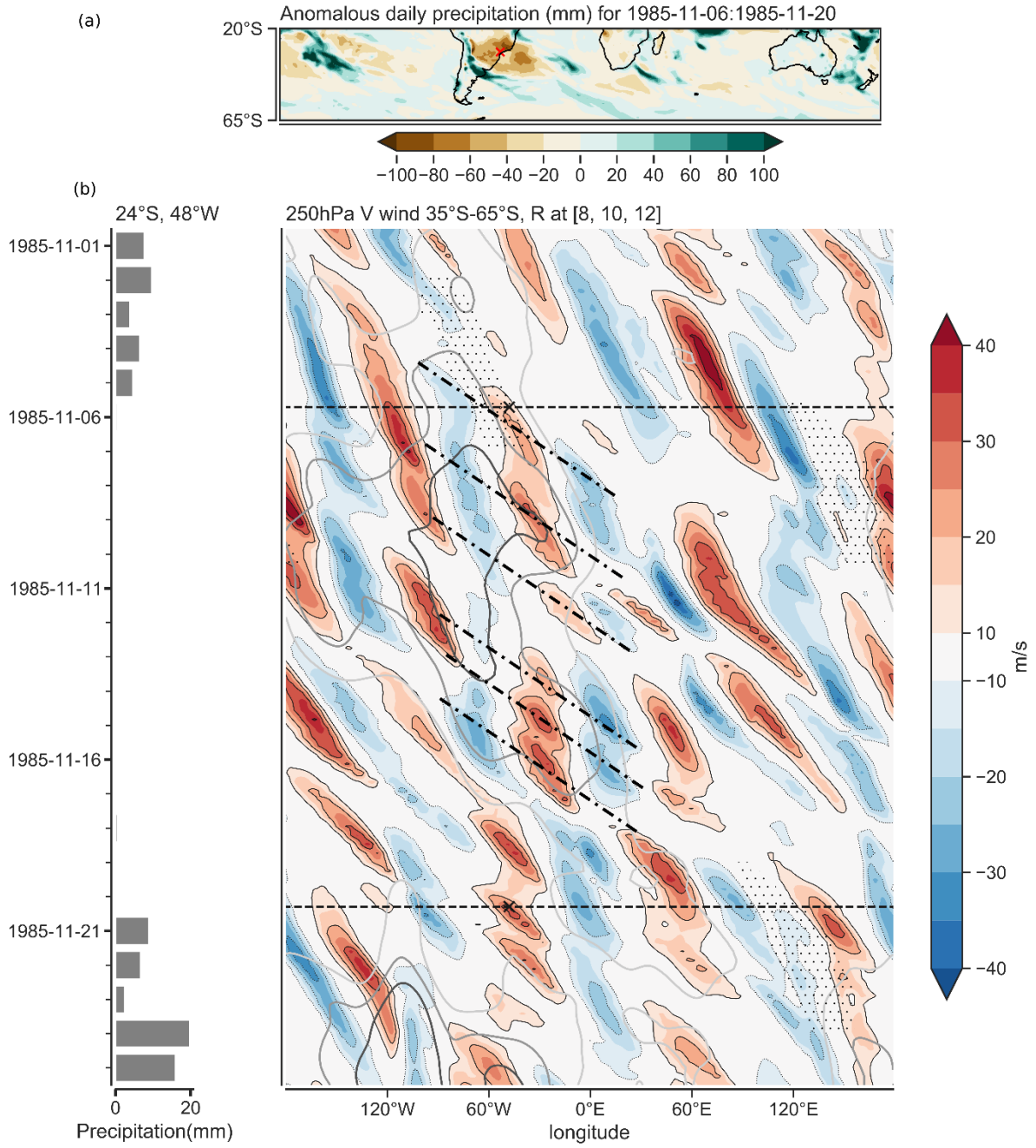

198

199 *Figure 2. (a) and (b) same as Figure 1 but for a dry spell event at 24°S, 48°W (Brazil) during November*
200 *1985. The Hovmöller diagram and the R-metric has been computed for 35°S-65°S.*

201

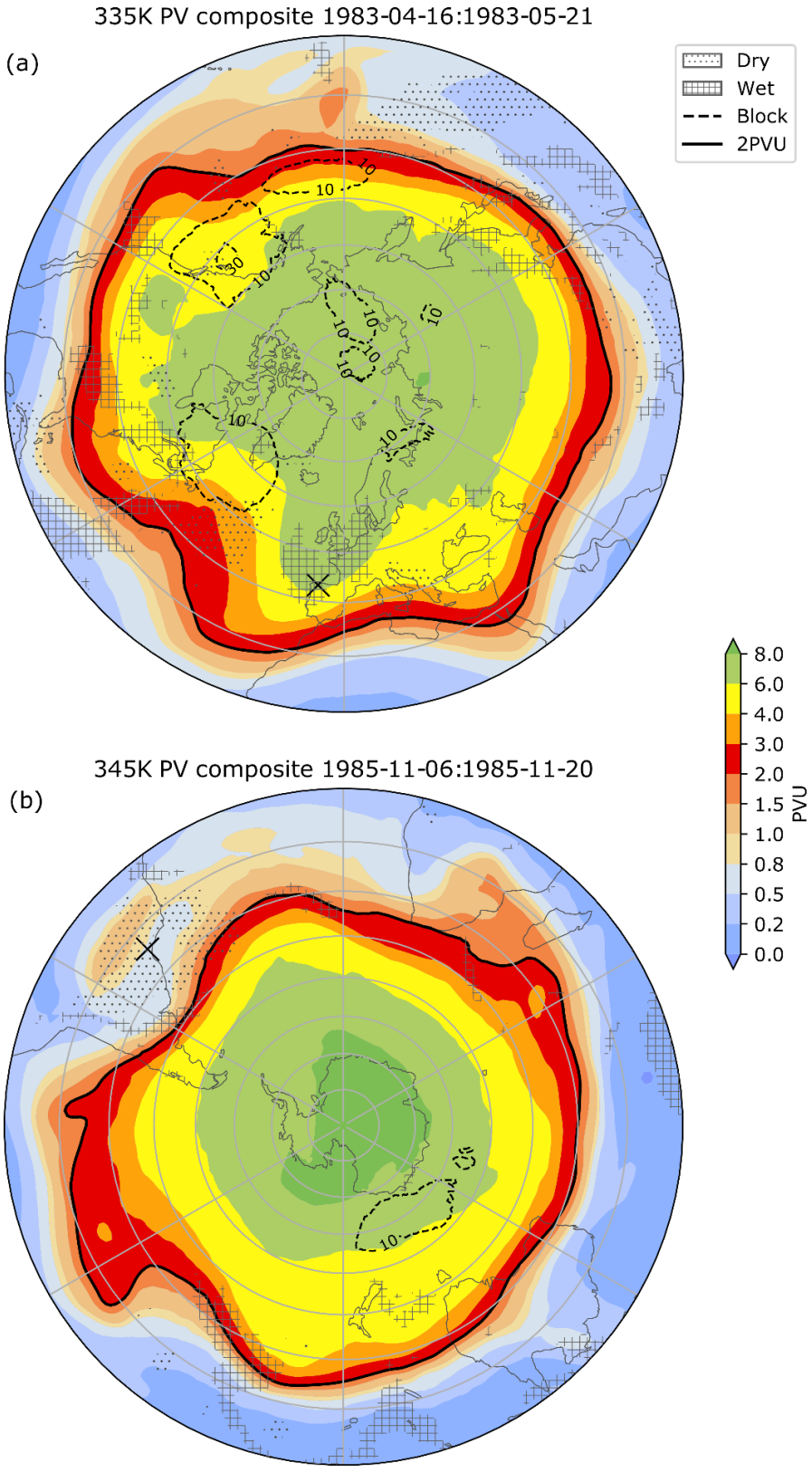

Figure 3. (a) PV at 335K isentrope averaged for the duration of wet spell in Figure 1. (b) Same as in (a) but at 345K isentrope for the duration of dry spell in Figure 2. Daily precipitation anomalies aggregated for the spell duration exceeding ± 40 mm are indicated by the corresponding hatches (see legend). 'X' shows location of spell duration. Dashed contours show blocking frequencies in percent.

3.2 Rossby wave recurrence associated with dry spells

Next, we present AF fields and begin with dry spells in the Northern Hemisphere. Recall that AF >1 (AF < 1) indicates a significant increase (decrease) of spell durations during RRWPs (i.e., for large values of R). Figures 4a and 4b show that RRWPs significantly affect the Northern Hemisphere dry spell durations during both the extended summer (MJJASO) and the winter (NDJFMA) seasons. However, this effect varies in sign depending on the region and the season. A positive effect of RRWPs on MJJASO dry spell durations is, for example, apparent in North America, central Europe, and eastern China (Figure 4a), while a negative effect is evident, for example, over western Greenland and numerous subtropical regions. Moreover, during MJJASO, some indication of a wave-like pattern is evident, in particular between 120°W and 60°E. During the NDJFMA (Figure 4b), significant Northern Hemisphere AF patterns have clear latitudinal structure, with widespread AF < 1 in the subtropics and the Arctic. Moreover, the mid-latitudes again feature a rather wave-like AF pattern again (approximately WN 4) in particular over the US and the Atlantic. Note that in both the seasons widespread AF > 1 regions are present in the mid-latitudes, but only in the southwestern US are AFs > 1 present during both seasons (Figures 4a and 4b).

Moving on to the Southern Hemisphere (SH) dry spells, we find that RRWPs significantly affect dry spell durations during MJJASO and NDJFMA, albeit more strongly during later (Figure 4). During NDJFMA, AFs > 1 are found over parts of subtropical South America, south-eastern Australia, and New Zealand, and AFs < 1 over parts of Patagonia, southern Africa, and northern and central Australia. Moreover, the majority of the AFs > 1 are present in the mid-latitudes. During MJJASO, however, the AF field shows a patchy structure, with coherent regions statistically significant AFs (<1) primarily in the subtropics and along the Antarctic coast.

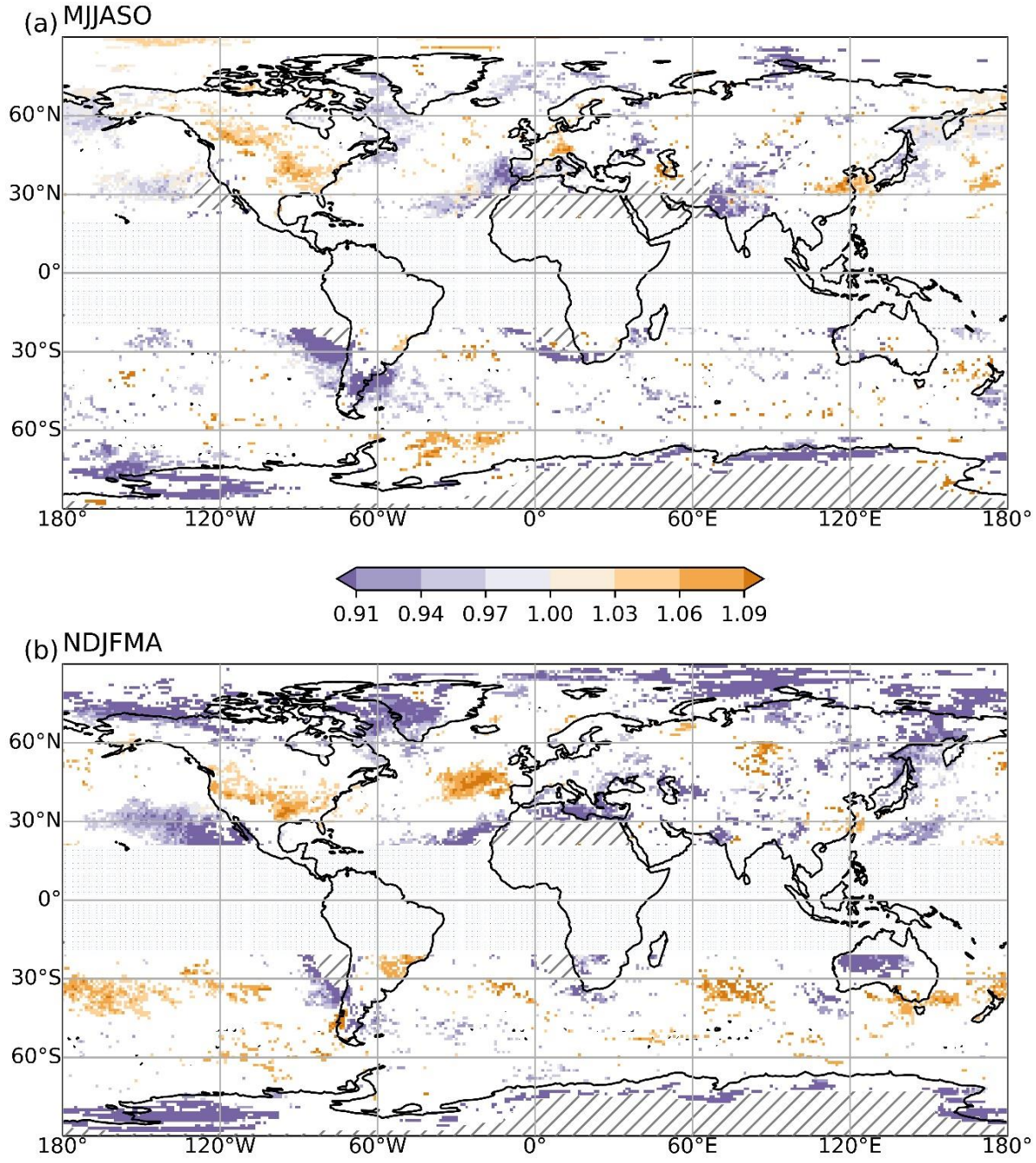

Figure 4. Statistically significant acceleration factors for (a) MJJASO and (b) NDJFMA dry spells. Northern Hemisphere (Southern Hemisphere) grid points show AFs from a Weibull model with the NH (SH) R-metric as a covariate, respectively. Lined hatches show areas excluded from the regression model. Stippling denotes areas where the null hypothesis that the spell durations are Weibull distributed, is rejected (only a few), based on Anderson-Darling test at significance level 0.01.

3.3 Rossby wave recurrence associated with wet spells

Similarly, for wet spell durations, the effect of RRWPs is dependent on the region and the season (Figure 5). In the NH, there are coherent regions with significantly longer wet spells during MJJASO in western Europe (France, Iberia) and western Russia (Figure 5a). In contrast to AFs for dry spells, for wet spells there are only few North American grid points with AFs significantly different from zero (cf. Figures 4a and 5a). During NDJFMA, RRWPs are associated with longer wet spells mainly over eastern Europe and the Mediterranean (Figure 5b), whereas large and reasonably coherent regions of AFs < 1 appear over the eastern North Atlantic (including Ireland, the UK) as well as over North-western Russia. Furthermore, no latitudinal structure in the wet-spell AFs is apparent in the Northern Hemisphere. However, note that many high-latitude and subtropical areas are excluded from this analysis due to too few wet spells.

In contrast, in the SH (Figure 5), the AF fields exhibit a clear latitudinal structure that is evident in both the seasons. The AF patterns indicate an increase of wet spell durations associated with RRWPs between 30°S and 50°S, and a decrease of wet spell durations associated with RRWPs south of 50°S. In particular, positive AF regions are apparent for both the seasons over subtropical South America and parts of New Zealand.

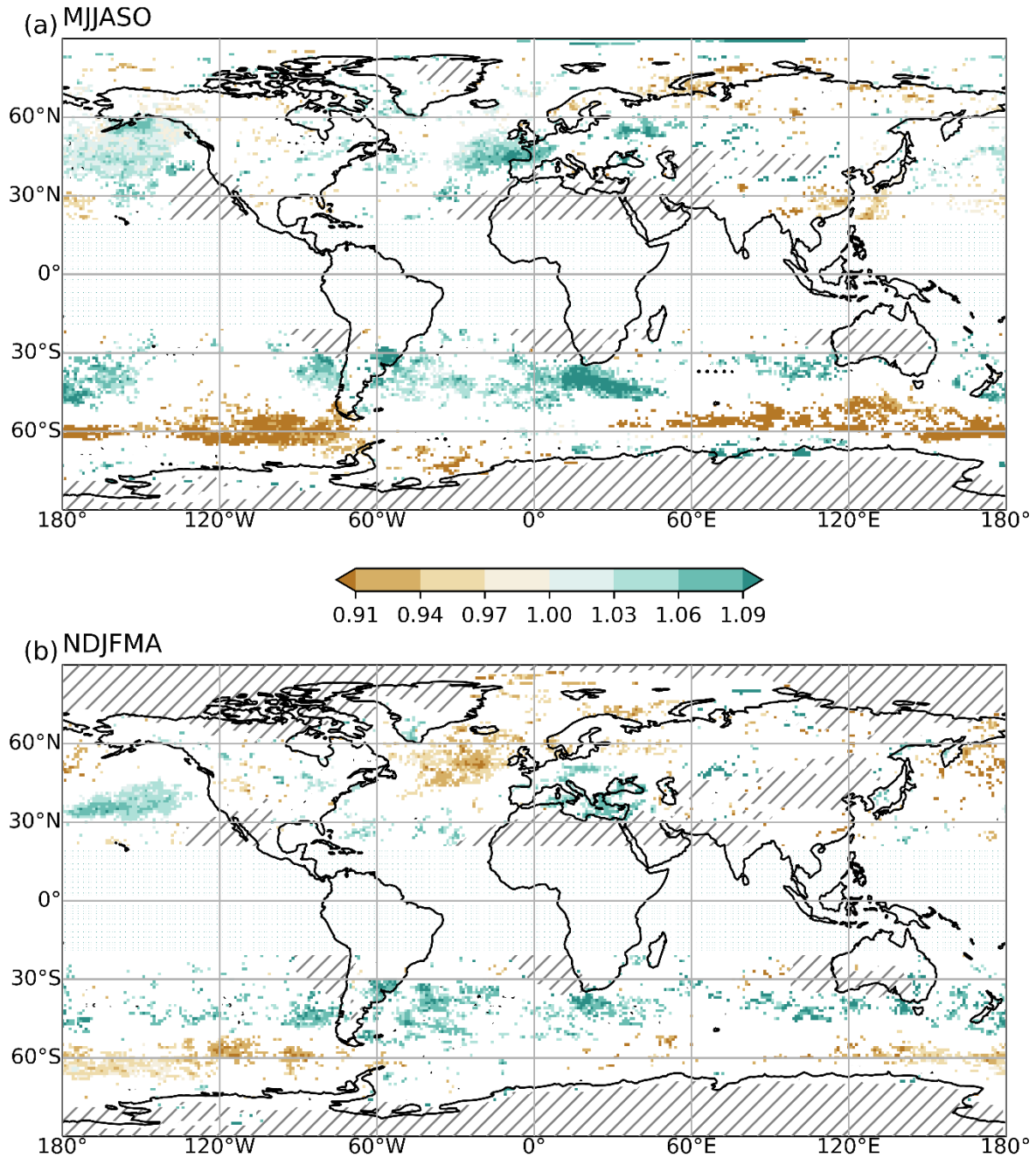

257

258 *Figure 5. Same as Figure 4 but for (a) MJJASO and (b) NDJFMA dry spells.*

259

4. Discussion

Our results demonstrate that recurrence of transient Rossby waves significantly affects the persistence of dry and wet spells. However, its effect can take either sign; it can both increase or decrease wet and dry spells.

Most regions where RRWPs are associated with a decrease in spell durations are regions where persistence is large climatologically, for example, in the subtropics and the Arctic for dry spells, and in the storm track regions for wet spells (refer median spell durations in Figures S2 and S4). This implies that the recurrent troughs and ridges can interrupt wet and dry periods in these regions and reduce persistence.

The AF patterns for wet and dry spells arise from a combination three components: a zonally symmetric component, a wave-like component, and a local component. The zonally symmetric component is most coherent in winter. It is characterized by distinct latitudinal bands in the AFs: with increased wet spell persistence on the equatorward side of the storm tracks (most evident in winter for NH Pacific and SH storm tracks), and reduced wet spell persistence in the central part of the storm tracks (both for NH Pacific and Atlantic, and SH storm tracks in winter). Furthermore, it features increased dry spell persistence in the central part of some storm tracks and reduced dry spell persistence in the subtropics and Arctic.

The zonally symmetric part can be understood by recalling that RRWPs are highly amplified flow situations. Hence, they lead to increased moisture transport into the polar regions and frequent RWB. The increased polar moisture transport can interrupt dry spells (e.g., Ali & Pithan, 2020; Papritz & Dunn-Sigouin, 2020; Uotila et al., 2013). Similarly, frequent RWB can foster unusually persistent wet conditions on the equatorward flank of the storm tracks (e.g., De Vries, 2020; De Vries et al., 2013) and interrupt dry spells by triggering convection (e.g., Funatsu & Waugh, 2008; McTaggert et al., 2008). Recurrent ridging in the central part of the storm tracks (which are climatologically very wet regions) can shorten wet spells there (Wernli and Schwierz, 2006). The zonally symmetric part has also been discussed in Röthlisberger et al. 2019 (their Figure 10a), but for persistent cold spells in winter.

The wave-like component in the AF fields is relevant for dry spells in the NH and is more evident during boreal winter (Figures 4b and 5b). A similar wave-like component has also been reported by Röthlisberger et al. 2019 (their Figure 10b) for NH hot spells during summer, having a wavenumber 6-7. However, there is no clear circumglobal wavenumber for the AF patterns of dry and wet spells. The presence of such a wave-like component in the AFs implies

that the RRWPs occur in preferred phases, i.e., the formation of troughs/ridges within RRWPs occurs in preferred geographical regions. In areas where RRWPs increase wet spell duration, potentially recurrent highly amplified upper-level troughs contribute to frequent precipitation along their downstream flank via quasi-geostrophic lifting. For example, the wet spell case in Spain during April-May 1983 described before, where recurrent troughs were present just east of the Iberian west coast (Figure 1 and 3a). Similarly, in areas where RRWPs are associated with longer dry spell durations, potentially recurrent upper-level ridges ensure dry and stable conditions (e.g., Figure 2 and 3b). Moreover, the lack of such a wave signal in the SH and the wavenumber dependence on the season suggests that the wave component in the AF fields is related to the stronger planetary waves in the NH that organise the transient eddies in preferred phases. However, note that the wave patterns should not be interpreted as occurring concomitantly and hence, as a circum-hemispheric wave. Although, such Rossby wave trains might exist but we cannot infer their presence from the AF patterns. It remains to be investigated to what extent this wave-like component in the AF field relates to Quasi Resonance Amplification, etc (Kornhuber et al., 2017).

Finally, the intricacies of local effects such as orography and moisture availability also affect AF patterns. For example, the case study shown in Figures 1 and 2 illustrates a long-lasting wet spell that is conceivably also affected by local orography. Furthermore, moisture transport is typically from the ocean towards the land and cannot cross major mountain ranges. This implies that local geography (coastline, mountain ranges, etc) play a role in determining whether a particular flow configuration is conducive to more/less persistent dry or wet spells.

5. Conclusions

Previously, mainly the stationary flow has been considered as an important driver of persistent weather conditions. Here, we demonstrate the importance of recurrent transient synoptic-scale Rossby wave packets (RRWPs) for persistent dry and wet conditions. RRWPs provide a non-stationary mechanism for modulating persistent surface weather. Röthlisberger et al. 2019 showed that RRWPs affect Northern Hemisphere temperature spells. Here, we demonstrate that RRWPs also significantly affect the duration of dry and wet spells globally by significantly shortening or extending the persistent dry/wet conditions. Spatial patterns of statistically significant regression coefficients feature superimposed components, a zonally symmetric component, and a wave-like component that are modulated by local effects, presumably arising from the local geography, such as orography or the position relative to major moisture sources. The zonally symmetric component is apparent during the Northern Hemisphere winter and

dominates the Southern Hemisphere signal in both the seasons. The wave-like component appears primarily in the Northern Hemisphere, changes its wavenumber with the season and is thus, conceivably related to stationary wave dynamics. Despite the regional variations in modulating wet/dry spell persistence, our results demonstrate that RRWPs significantly alter the persistence of potentially high-impact surface weather; RRWPs should, therefore, be considered as an essential flow feature for understanding and predicting persistent sub-seasonal weather patterns.

6. Acknowledgments and Data

We would like to acknowledge the Swiss National Science Foundation grant number 178751, ERA-I reanalysis data (Dee et al, 2011), and open source Python packages (Hoyer & Hamman, 2017; Hunter 2007; Kluyver 2016). Datasets created in this study are available from FAIR-aligned repository in the in-text data citation Ali (2020).

7. References

Ali, S. M., (2020). Dataset for Recurrent Rossby wave packets modulate the persistence of dry and wet spells across the globe (Version 1) [Data set]. *Zenodo*. doi:10.5281/zenodo.4134145

Ali, S. M., & Pithan, F. (2020). Following moist intrusions into the Arctic using SHEBA observations in a Lagrangian perspective. *Quarterly Journal of the Royal Meteorological Society,* 1–18. https://doi.org/10.1002/qj.3859

Barton, Y., Giannakaki, P., von Waldow, H., Chevalier, C., Pfahl, S., & Martius, O. (2016). Clustering of Regional-Scale Extreme Precipitation Events in Southern Switzerland. *Monthly Weather Review*. https://doi.org/10.1175/MWR-D-15-0205.1

Blackburn, M., Methven, J., & Roberts, N. (2008). Large-scale context for the UK floods in summer 2007. *Weather*, *63*(9), 280–288. https://doi.org/10.1002/wea.322

Coumou, D., Petoukhov, V., Rahmstorf, S., Petri, S., & Schellnhuber, H. J. (2014). Quasi-resonant circulation regimes and hemispheric synchronization of extreme weather in boreal summer. *Proceedings of the National Academy of Sciences*. https://doi.org/10.1073/pnas.1412797111

Davies, H. C. (2015). Weather chains during the 2013/2014 winter and their significance for seasonal prediction. *Nature Geoscience*, *8*(11), 833–837. https://doi.org/10.1038/ngeo2561

De Vries, A. J., Tyrlis, E., Edry, D., Krichak, S. O., Steil, B., and Lelieveld, J. (2013), Extreme precipitation events in the Middle East: Dynamics of the Active Red Sea Trough, *Journal of Geophysical Research Atmosphere*, 118, 7087– 7108, doi:10.1002/jgrd.50569.

De Vries, A. J. (2020). A global climatological perspective on the importance of Rossby wave breaking and intense moisture transport for extreme precipitation events. *Weather Climate Dynamics Discussion*, https://doi.org/10.5194/wcd-2020-44, in review.

Dee, D. P., Uppala, S. M., Simmons, A. J., Berrisford, P., Poli, P., Kobayashi, S., et al. (2011). The ERA-Interim reanalysis: Configuration and performance of the data assimilation system. *Quarterly Journal of the Royal Meteorological Society*, *137*(656), 553–597. https://doi.org/10.1002/qj.828

Drouard, M., & Woollings, T. (2018). Contrasting Mechanisms of Summer Blocking Over Western Eurasia. *Geophysical Research Letters*, *45*(21), 12,040-12,048. https://doi.org/10.1029/2018GL079894

Fang, Y., Chen, W., & Zhou, W. (2012). Analysis of the role played by circulation in the persistent precipitation over South China in June 2010. *Advances in Atmospheric Sciences*, *29*(4), 769–781. https://doi.org/10.1007/s00376-012-2018-7

Fang, B., & Lu, M. (2020). Heatwave and blocking in the Northeastern Asia: Occurrence, variability, and association. *Journal of Geophysical Research: Atmospheres, 125*, e2019JD031627. https://doi.org/10.1029/2019JD031627

Funatsu, B. M., & D. W. Waugh. (2008). Connections between potential vorticity intrusions and convection in the eastern tropical pacific. *Journal of Atmospheric Science, 65*, 987-1002. https://doi.org/10.1175/2007JAS2248.1

Ferranti, L., Corti, S. & Janousek, M. (2015), Flow-dependent verification of the ECMWF ensemble over the Euro-Atlantic sector. *Quarterly Journal of the Royal Meteorological Society, 141:* 916-924. https://doi.org/10.1002/qj.2411

Hoyer, S. & Hamman, J., (2017). xarray: N-D labeled Arrays and Datasets in Python. *Journal of Open Research Software*. 5(1), p.10. DOI: http://doi.org/10.5334/jors.148

Hosmer, D. W., Lemeshow, S., & May, S. (2008). Applied Survival Analysis. 2nd ed., Wiley Series in Probability and Statistics, *John Wiley & Sons, Inc*. 416 pp. https://doi.org/10.1002/9780470258019

Hunter, J. D. (2007). Matplotlib: A 2D Graphics Environment, *Computing in Science & Engineering*, 9(3), pp. 90-95. https://doi.org/10.1109/MCSE.2007.55

Kluyver, T., Ragan-Kelley, B., Pérez, F., Granger, B. E., Bussonnier, M., Frederic, J., ... & Ivanov, P. (2016). Jupyter Notebooks-a publishing format for reproducible computational workflows. In ELPUB (pp. 87-90). doi: 10.3233/978-1-61499-649-1-87

Kornhuber, K., Petoukhov, V., Petri, S., Rahmstorf, S., & Coumou, D. (2016). Evidence for wave resonance as a key mechanism for generating high-amplitude quasi-stationary waves in boreal summer. *Climate Dynamics*. https://doi.org/10.1007/s00382-016-3399-6

Kornhuber, K., V. Petoukhov, D. Karoly, S. Petri, S. Rahmstorf, & D. Coumou (2017).

Summertime Planetary Wave Resonance in the Northern and Southern Hemispheres. *Journal of Climate*, 30, 6133-6150. http://journals.ametsoc.org/doi/10.1175/JCLI-D-16-0703.1

Kornhuber, K., Coumou, D., Vogel, E., Lesk, C., Donges, J. F., Lehmann, J., & Horton, R. M. (2020). Amplified Rossby waves enhance risk of concurrent heatwaves in major breadbasket regions. *Nature Climate Change, 10*(1), 48–53. https://doi.org/10.1038/s41558-019-0637-z

Lenggenhager, S., Croci-Maspoli, M., Brönnimann, S., & Martius, O. (2019). On the dynamical coupling between atmospheric blocks and heavy precipitation events: A discussion of the southern Alpine flood in October 2000. *Quarterly Journal of the Royal Meteorological Society, 145*(719), 530–545. https://doi.org/10.1002/qj.3449

Li, M, Luo, D, Yao, Y, Zhong, L. (2020). Large-scale atmospheric circulation control of summer extreme hot events over China. *International Journal of Climatology, 40*: 1456– 1476. https://doi.org/10.1002/joc.6279

Matsueda, M. & Palmer, T. N. (2018). Estimates of flow-dependent predictability of wintertime Euro-Atlantic weather regimes in medium-range forecasts. *Quaterly Journal of Royal Meteorological Society, 144*, 1012– 1027. https://doi.org/10.1002/qj.3265

McTaggart-Cowan, R., T. J. Galarneau, L. F. Bosart, R. W. Moore, & O. Martius (2013). A Global Climatology of Baroclinically Influenced Tropical Cyclogenesis. *Monthly Weather Review*, *141***,** 1963-1989. https://doi.org/10.1175/MWR-D-12-00186.1

Michelangeli, P.-A., Vautard, R., & Legras, B. (1995). Weather Regimes: Reccurrence and Quasi Stationarity. *American Meteorological Society*. https://doi.org/10.1175/1520-0469(1995)052<1237:WRRAQS>2.0.CO;2.

Quandt, L., J. H. Keller, O. Martius, and S. C. Jones (2017). Forecast Variability of the Blocking System over Russia in Summer 2010 and Its Impact on Surface Conditions. *Weather Forecasting, 32, 61–82*, https://doi.org/10.1175/WAF-D-16-0065.1.

Papritz, L., & Dunn-Sigouin, E. (2020). What configuration of the atmospheric circulation drives extreme net and total moisture transport into the Arctic? *Geophysical Research Letters*. https://doi.org/10.1029/2020GL089769

Pelly, J. L., & Hoskins, B. J. (2003). A new perspective on blocking. *Journal of the*

Atmospheric Sciences, *60*(5), 743-755. https://doi.org/10.1175/1520-0469(2003)060<0743:ANPOB>2.0.CO;2

Pfahl, S., & Wernli, H. (2012). Quantifying the relevance of atmospheric blocking for co-located temperature extremes in the Northern Hemisphere on (sub-)daily time scales. *Geophysical Research Letters*, *39*(12), 1–6. https://doi.org/10.1029/2012GL052261

Quinting, J. F., Parker, T. J., & Reeder, M. J. (2018). Two synoptic routes to subtropical heat waves as illustrated in the Brisbane region of Australia. *Geophysical Research Letters*, 45, 10,700– 10,708. https://doi.org/10.1029/2018GL079261

Raymond, C., Horton, R. M., Zscheischler, J., Martius, O., Aghakouchak, A., Balch, J., et al. (2020). extreme events. *Nature Climate Change*. https://doi.org/10.1038/s41558-020-0790-4

Rex, D. F. (1950). Blocking action in the middle troposphere and its effect upon regional climate. Tellus, 2(4), 275-301. https://doi.org/10.3402/tellusa.v2i4.8603

Rhodes, R. I. (2017). Clustering and stalling of North Atlantic cyclones: the influence on precipitation in England and Wales *(Doctoral dissertation, University of Reading*). http://centaur.reading.ac.uk/77911/

Risser, M. D., & Wehner, M. F. (2017). Attributable Human-Induced Changes in the Likelihood and Magnitude of the Observed Extreme Precipitation during Hurricane Harvey. *Geophysical Research Letters*, *44*(24), 12,457-12,464. https://doi.org/10.1002/2017GL075888

Rohrer, M., Brönnimann, S., Martius, O., Raible, C. C., Wild, M., & Compo, G. P. (2018). Representation of extratropical cyclones, blocking anticyclones, and alpine circulation types in multiple reanalyses and model simulations. *Journal of Climate*, *31*(8), 3009–3031. https://doi.org/10.1175/JCLI-D-17-0350.1

Röthlisberger, M., Frossard, L., Bosart, L. F., Keyser, D., & Martius, O. (2019a). Recurrent synoptic-scale Rossby wave patterns and their effect on the persistence of cold and hot spells. *Journal of Climate*, *32*(11), 3207–3226. https://doi.org/10.1175/JCLI-D-18-0664.1

Röthlisberger, M., & Martius, O. (2019b). Quantifying the Local Effect of Northern Hemisphere Atmospheric Blocks on the Persistence of Summer Hot and Dry Spells.

Geophysical Research Letters, *46*(16), 10101–10111. https://doi.org/10.1029/2019gl083745

Rudd, A. C., Kay, A. L., Wells, S. C., Aldridge, T., Cole, S. J., Kendon, E. J., & Stewart, E. J. (2020). Investigating potential future changes in surface water flooding hazard and impact. *Hydrological Processes*, *34*(1), 139–149. https://doi.org/10.1002/hyp.13572

Schaller, N., Kay, A. L., Lamb, R., Massey, N. R., Van Oldenborgh, G. J., Otto, F. E. L., et al. (2016). Human influence on climate in the 2014 southern England winter floods and their impacts. *Nature Climate Change*, *6*(6), 627–634. https://doi.org/10.1038/nclimate2927

Schwierz, C., Croci-Maspoli, M., and Davies, H. C. (2004). Perspicacious indicators of atmospheric blocking, *Geophysical Research Letters*, *31*, L06125, doi:10.1029/2003GL019341.

Sivakumar, M. V. (2018). Climate Extremes and Impacts on Agriculture. *Agroclimatology: Linking Agriculture to Climate*, *60*, 621–647. https://doi.org/10.2134/agronmonogr60.2018.0006

Stadtherr, L., Coumou, D., Petoukhov, V., Petri, S., & Rahmstorf, S. (2016). Record Balkan floods of 2014 linked to planetary wave resonance. *Science Advances*, *2*(4), 1–7. https://doi.org/10.1126/sciadv.1501428

Uotila, P., Vihma, T., & Tsukernik, M. (2013). Close interactions between the Antarctic cyclone budget and large-scale atmospheric circulation. *Geophysical Research Letters*, *40*(12), 3237–3241. https://doi.org/10.1002/grl.50560

Webster, P. J., Toma, V. E., and Kim, H. M. (2011), Were the 2010 Pakistan floods predictable? *Geophysical Research Letters, 38*, L04806, doi:10.1029/2010GL046346.

Wernli, H., & Schwierz, C. (2006). Surface cyclones in the ERA-40 dataset (1958-2001). Part I: Novel identification method and global climatology. *Journal of the Atmospheric Sciences*, *63*(10), 2486–2507. https://doi.org/10.1175/JAS3766.1

Wolf, G., Brayshaw, D. J., Klingaman, N. P., & Czaja, A. (2018). Quasi-stationary waves and their impact on European weather and extreme events. *Quarterly Journal of the Royal Meteorological Society*, *144*(717). https://doi.org/10.1002/qj.3310

Wolter, K., Hoerling, M., Eischeid, J. K., Van Oldenborgh, G. J., Quan, X. W., Walsh, J. E.,

et al. (2015). How unusual was the cold winter of 2013/14 in the upper midwest? *Bulletin of the American Meteorological Society*, *96*(12), S10–S14. https://doi.org/10.1175/BAMS-D-15-00126.1

Xu, P., Wang, L., Liu, Y., Chen, W., & Huang, P. (2020). The record-breaking heat wave of June 2019 in Central Europe. *Atmospheric Science Letters*, *21*(4), 1–7. https://doi.org/10.1002/asl.964

Zhang, Z. (2016). Parametric regression model for survival data: Weibull regression model as an example. *Annals of Translational Medicine*, *4*(24). https://doi.org/10.21037/atm.2016.08.45

Zschenderlein, P., Fragkoulidis, G., Fink, A. H., & Wirth, V. (2018). Large-scale Rossby wave and synoptic-scale dynamic analyses of the unusually late 2016 heatwave over Europe. *Weather*, *73*(9), 275–283. https://doi.org/10.1002/wea.3278

Zschenderlein, P., Pfahl, S., Wernli, H., and Fink, A. H. (2020). A Lagrangian analysis of upper-tropospheric anticyclones associated with heat waves in Europe, *Weather Climate Dynamics*, 1, 191–206. https://doi.org/10.5194/wcd-1-191-2020.

Geophysical Research Letters

Supporting Information for

Recurrent Rossby wave packets modulate the persistence of dry and wet spells across the globe

S. Mubashshir Ali[1], Olivia Martius[1,2], Matthias Röthlisberger[3]

[1]Oeschger Centre for Climate Change Research and Institute of Geography, University of Bern, Bern, Switzerland

[2]Mobiliar Lab for Natural Risks, University of Bern, Bern, Switzerland

[3]Institute for Atmospheric and Climate Science, ETH Zürich, Zürich, Switzerland

Corresponding author: S. Mubashshir Ali (mubashshir.ali@giub.unibe.ch)

1. Spell count and median for Dry Spells and Wet Spells

Figures S1 and S2 show spell counts and the median spell duration for dry spells where each spell has a minimum duration of 5 days. The yellow solid contours, showing regions having fewer than 40 dry spells, are excluded from our analysis. These are either the arid regions in the subtropics and poles, which have long running dry spells, or the wet regions in the tropics, where it rains too often to have 40 dry spells having a minimum duration of 5 days in a season. These regions are excluded from the regression model analysis. Thus, they appear as hatches in the Figures showing the acceleration factors (Figures 4 and 5).

Similarly, Figures S3 and S4 show spell counts and the median spell duration for wet spells where each spell has a minimum duration of 5 days. Several areas in the subtropical and the polar region are usually dry, and thus have fewer than 40 wet spells and are excluded from the analysis. In the tropics, the median wet spell duration is longest (Figure S4). The stormtrack regions of both the Northern and the Southern Hemisphere experience long wet spells during their respective winter seasons.

2. Additional examples of RRWPs and persistent dry and wet spells

2.1 A dry spell in North America

A 37-day long dry spell started on 28 August 1990 at 50°N 110°W, Canada. During the first 2-weeks high R values are present over and around 110°W, where several trough-ridge couplets amplify recurrently as shown in Figure S5. Noticeably, no blocking is directly present over this grid-point during the entire episode. There is also a consistent high R signal and recurrence of wave packets over the western Pacific Ocean as well as blocking. The PV composite (Figure S6) for this episode shows a wave extending from the western Pacific over to the Atlantic and into Europe. The flow over Asia and eastern Pacific is rather zonal. The PV composite indicates anticyclonic wave breaking over the Gulf of Alaska. There are also several blocks present south of Alaska during this period as shown by the blocking frequency contours.

2.2 A wet spell in South America

9 June 2006 marks the start of a 9-day long wet spell at 50°S and 55°W. The daily precipitation time series shows 9 consecutive days of precipitation. The Hovmöller diagram shows recurrent troughs leading to anomalous rainfall over parts of southern Brazil and Uruguay. The PV composite for this period (Figure S8) also shows a prominent trough over subtropical South America. In the PV composite wavenumber 6 structure is visible; however, the flow is considerably more zonal compared to the PV composite for the dry spell case over Iberia (Figure 3a). There are also two blocks situated over Indian Ocean and Pacific Ocean during this period, with the later block being present for around 60% of time during this event.

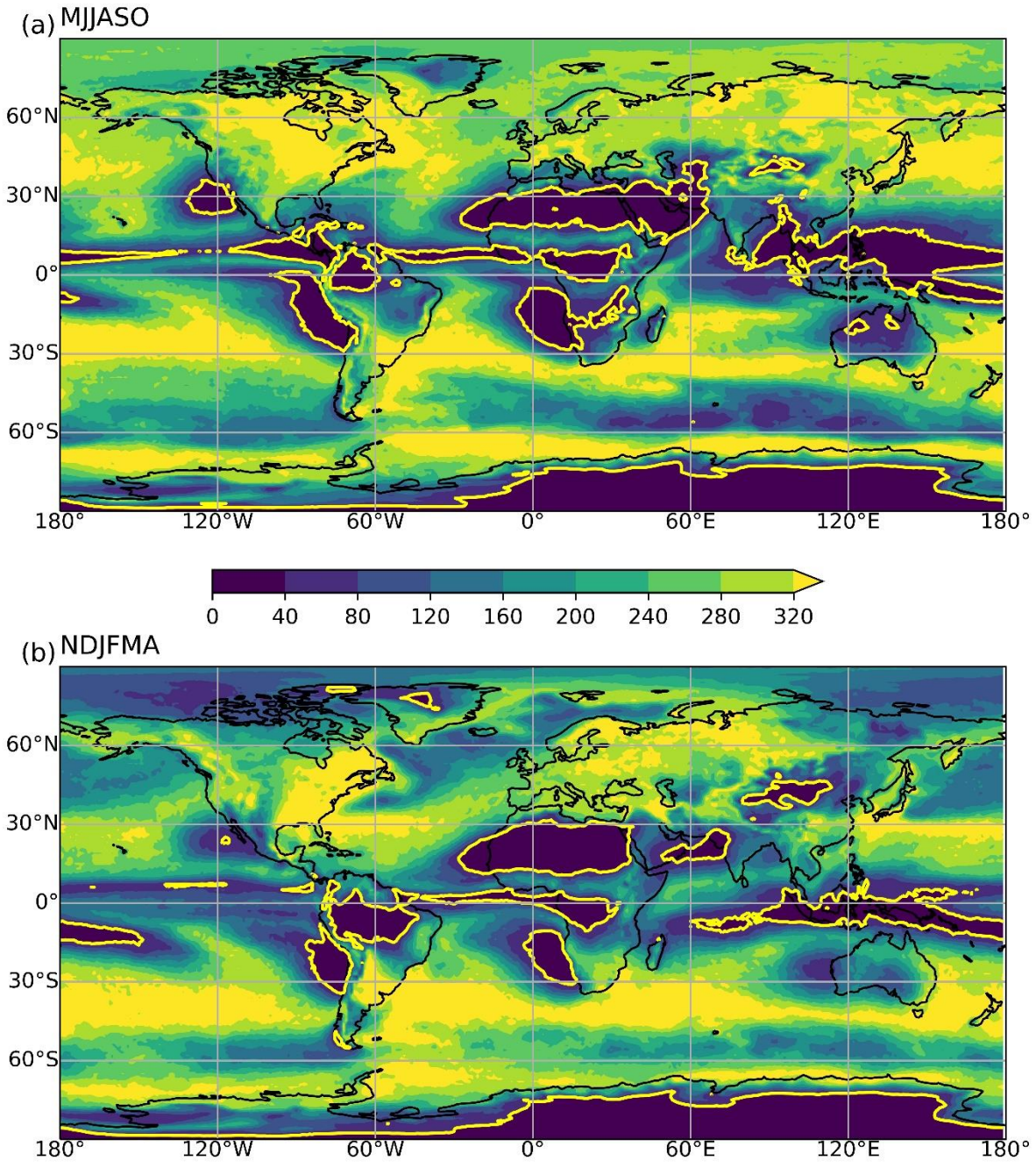

S1. Total number of MJJASO and NDJFMA dry spells (color shading) having a minimum spell length of 5 days. Solid yellow contours show areas with fewer than 40 spells between 1980-2016.

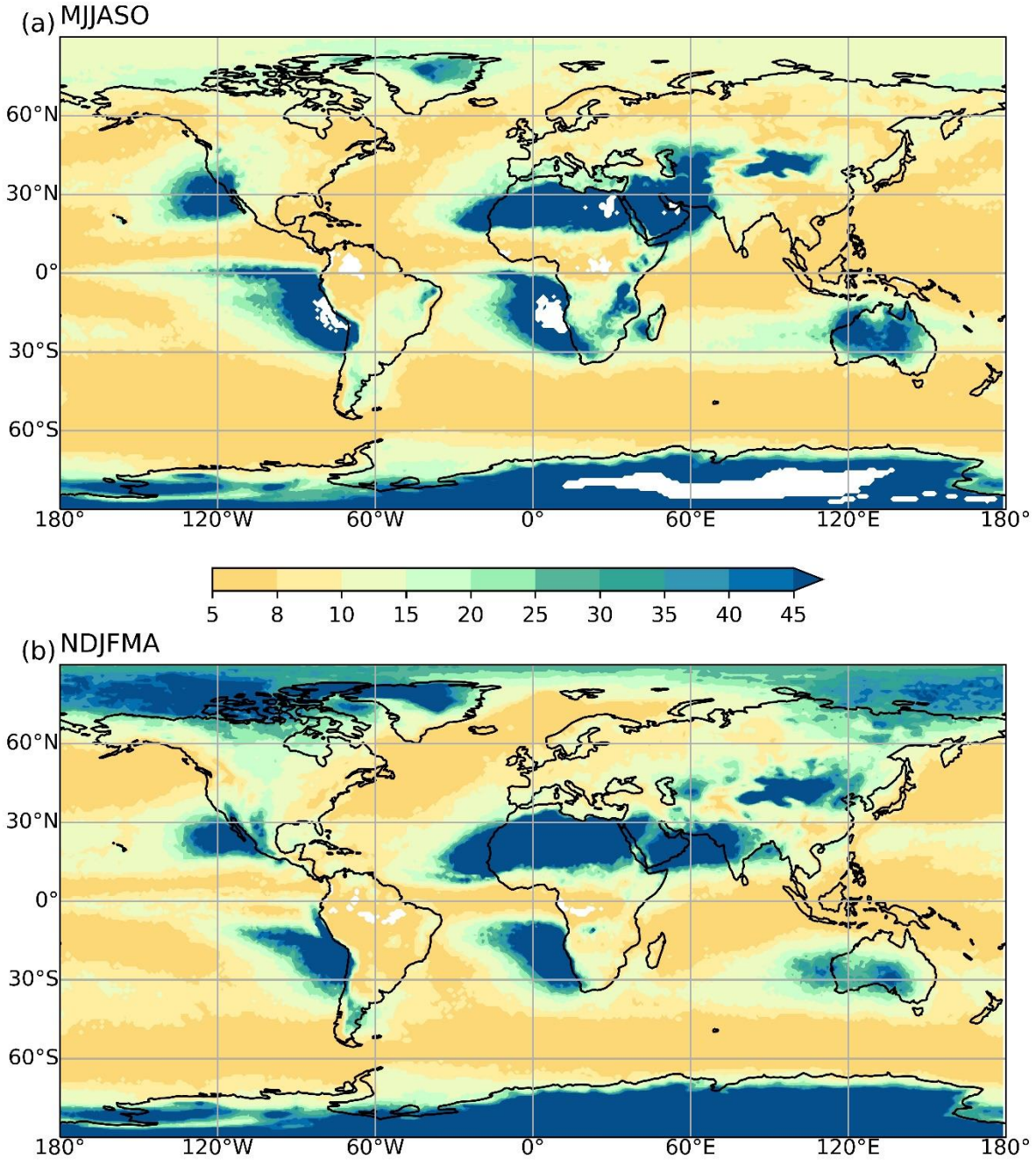

S2. Median MJJASO and NDJFMA dry spell length (color shading) for areas having a minimum spell duration of 5 days.

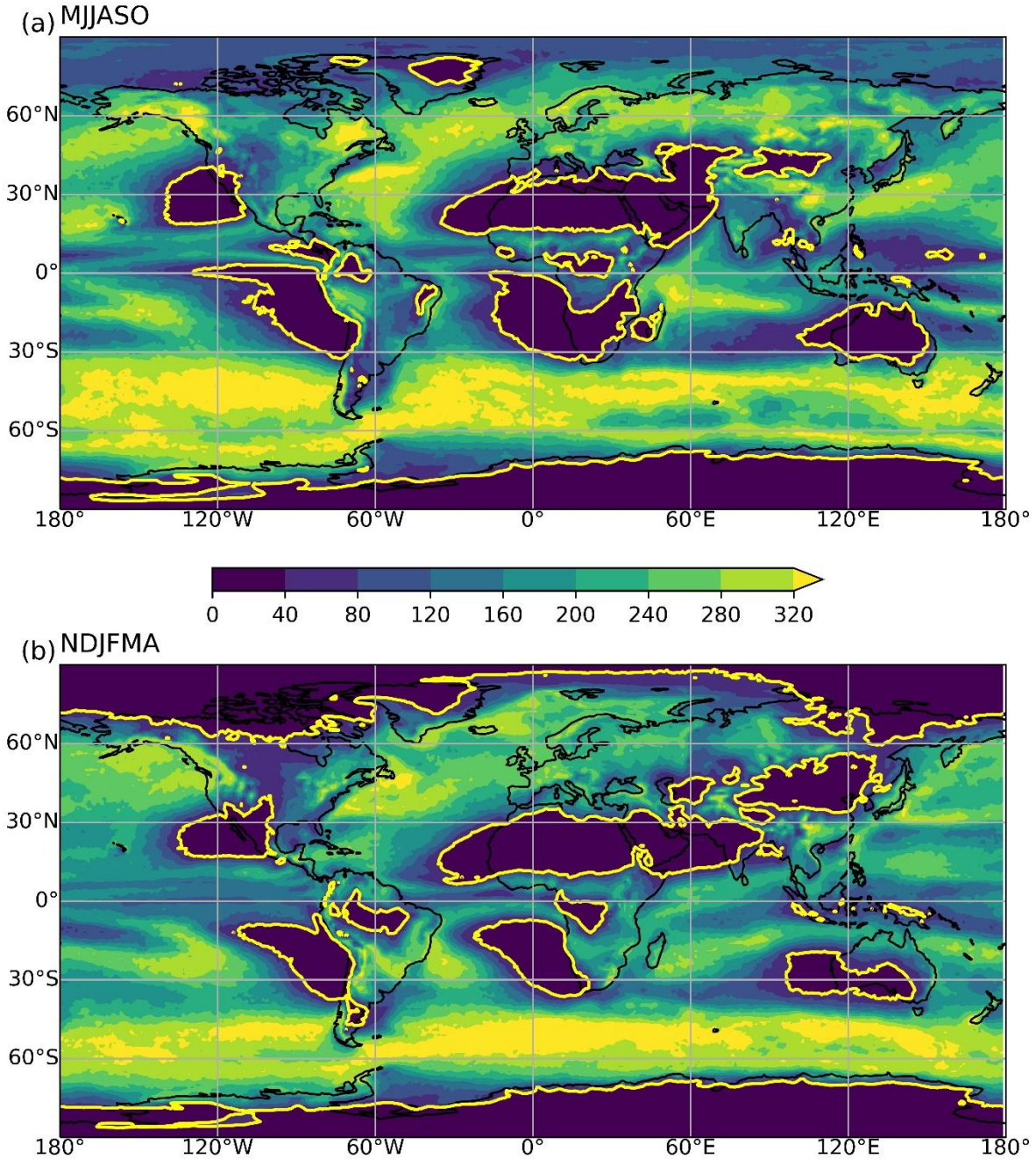

S3. Same as S1 except for MJJASO and NDJFMA wet spells.

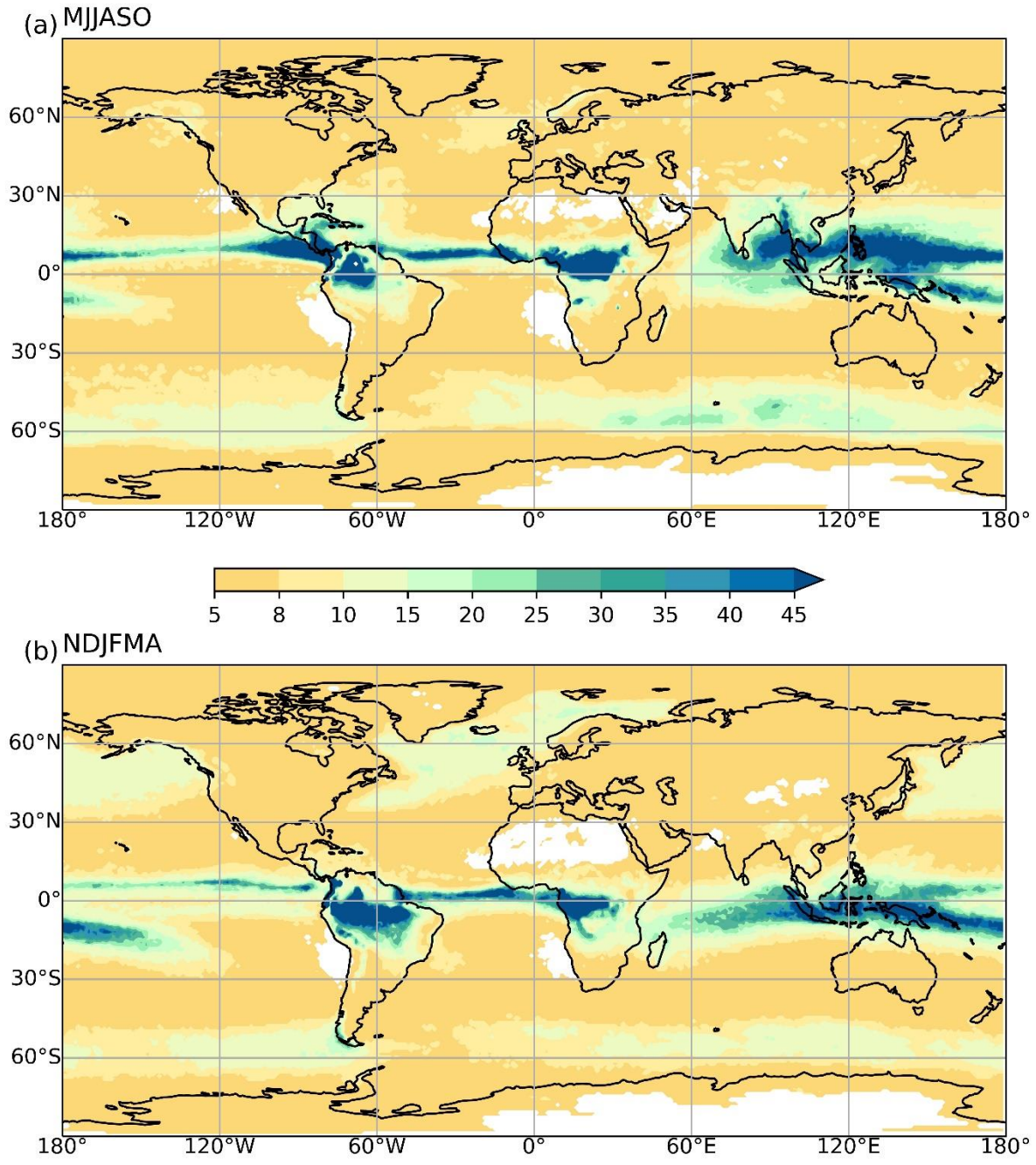

S4. Same as S2 except for MJJASO and NDJFMA wet spells.

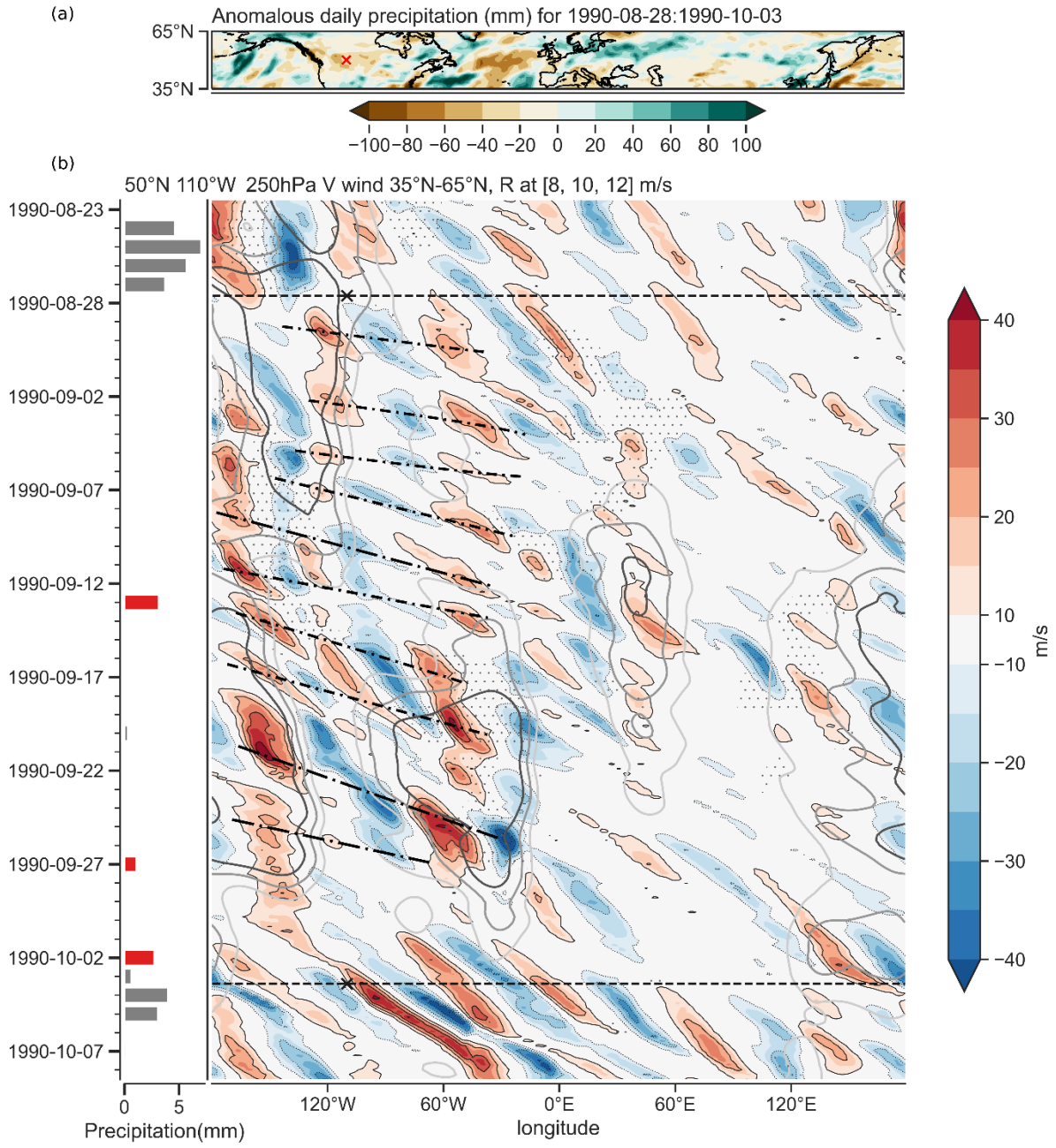

63

64 *S5. Dry spell during Aug-Sept 1990 over Canada and Northern US (a) Anomalous daily precipitation*
65 *(mm) compared to ERA-I climatology (1979-2018) for the same period. (b) Bars show aggregated daily*
66 *precipitation at location 'x' (50°N, 110°W) in (a), red when precipitation is in the spell period and*
67 *above 1 mm threshold, else grey. The Hovmöller diagram in (b) shows 35°N-65°N averaged meridional*
68 *wind at 250 hPa. Black dotted lines in (b) mark the onset and end of the spell at 'x' in (a). Grey contours*
69 *show R values of 8, 10, 12 m/s. Stipplings depicts longitudes at which at least one grid point in 20°N-*
70 *70°N featured an atmospheric block while the dash-dotted lines indicate the approximate longitude–*
71 *time trajectory of the Rossby wave packets (i.e., group propagation).*

72

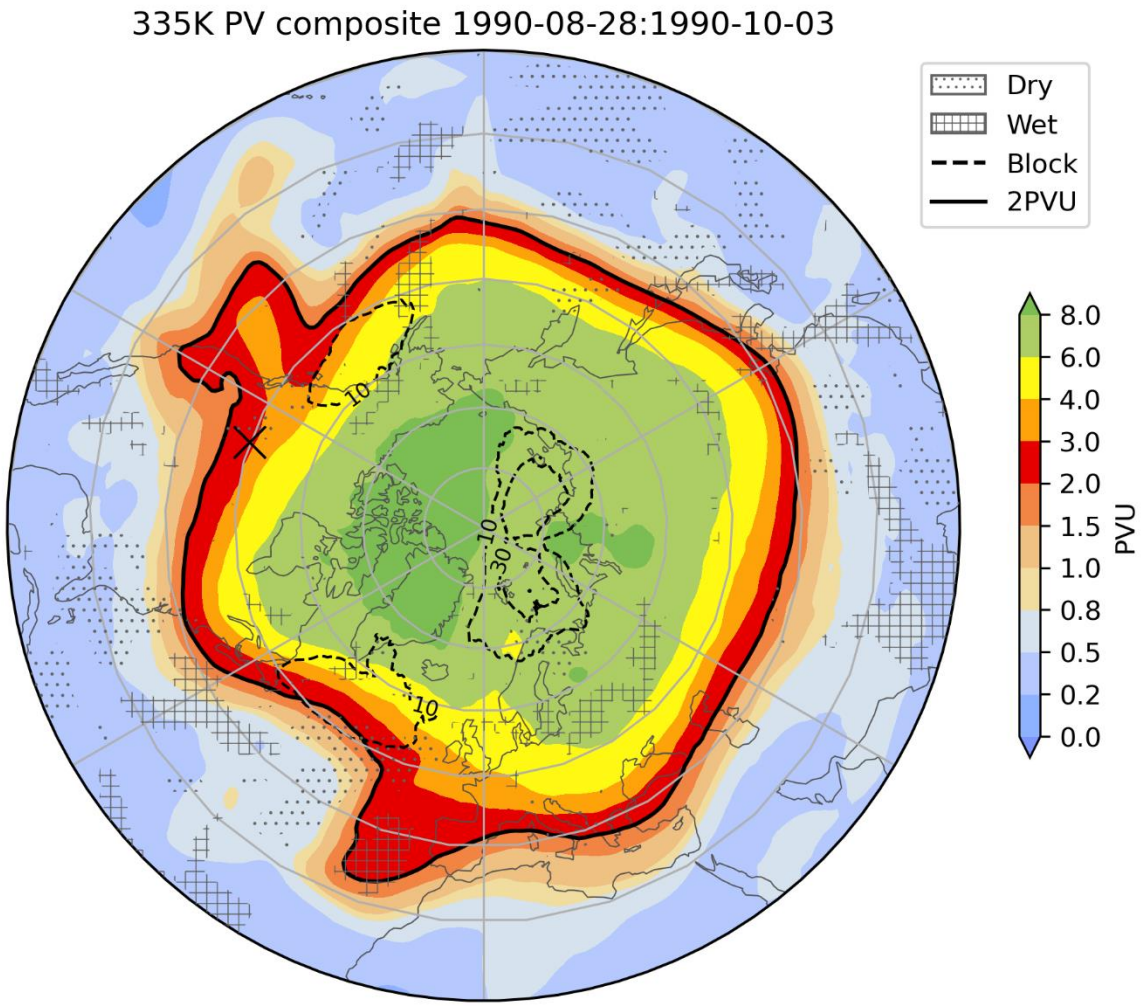

S6. PV at 335 K isentrope averaged for the spell duration in S5. Dashed contours indicate blocking frequency in %. Daily precipitation anomalies aggregated for the spell duration which exceed ±40 mm are indicated by the corresponding hatches (see legend).

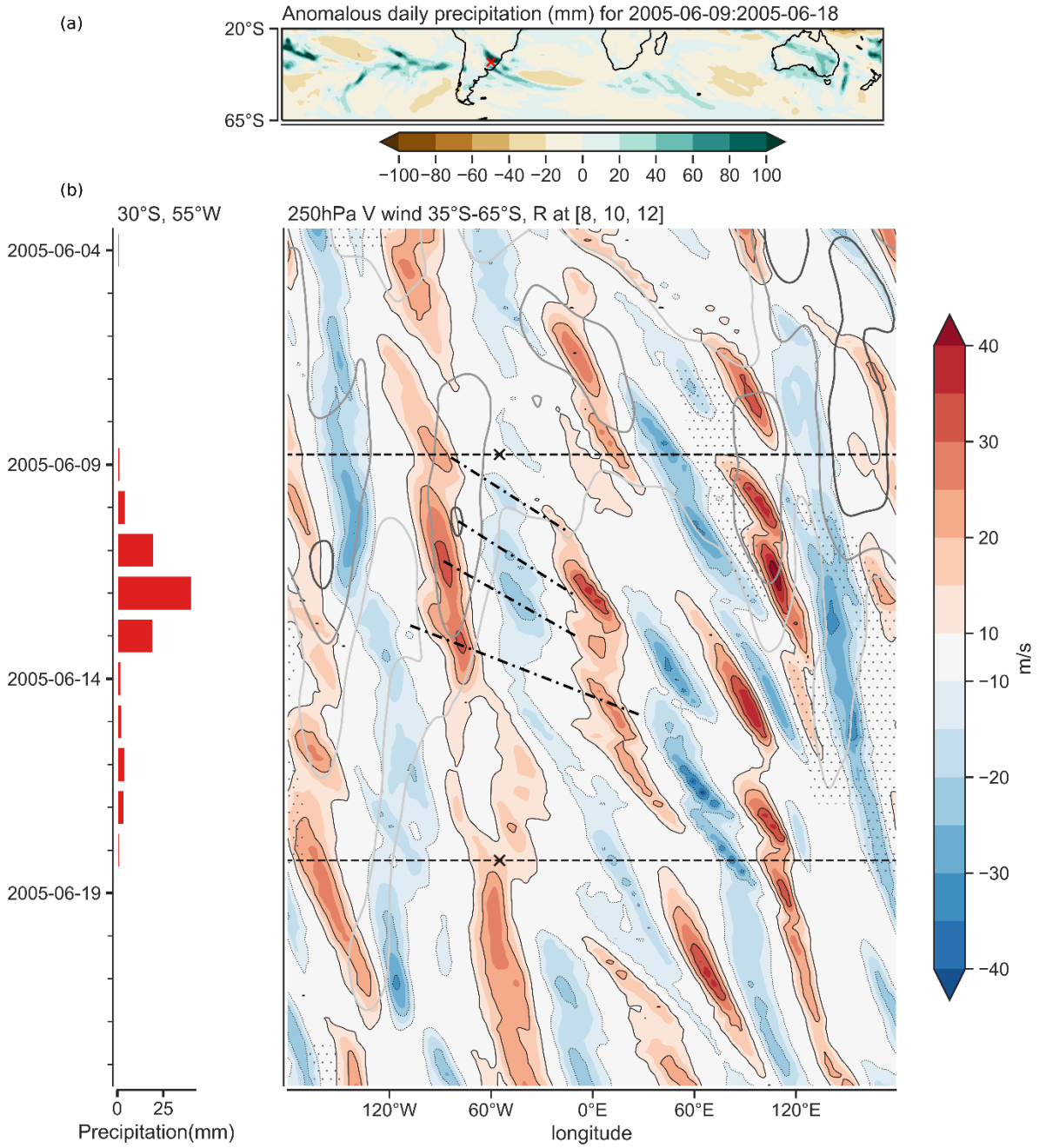

78

79 *S7. Same as S5 but for a wet spell over Southern Brazil (30°S, 55°W) during June 2005. The Hovmöller*
80 *diagram shows mean meridional wind at 250 hPa between 35°S-65°S in (b). Grey contours show R*
81 *values at 8, 10, 12 m/s. Stipplings depicts longitudes at which at least one grid point in 20°S-70°S*
82 *featured an atmospheric block.*

83

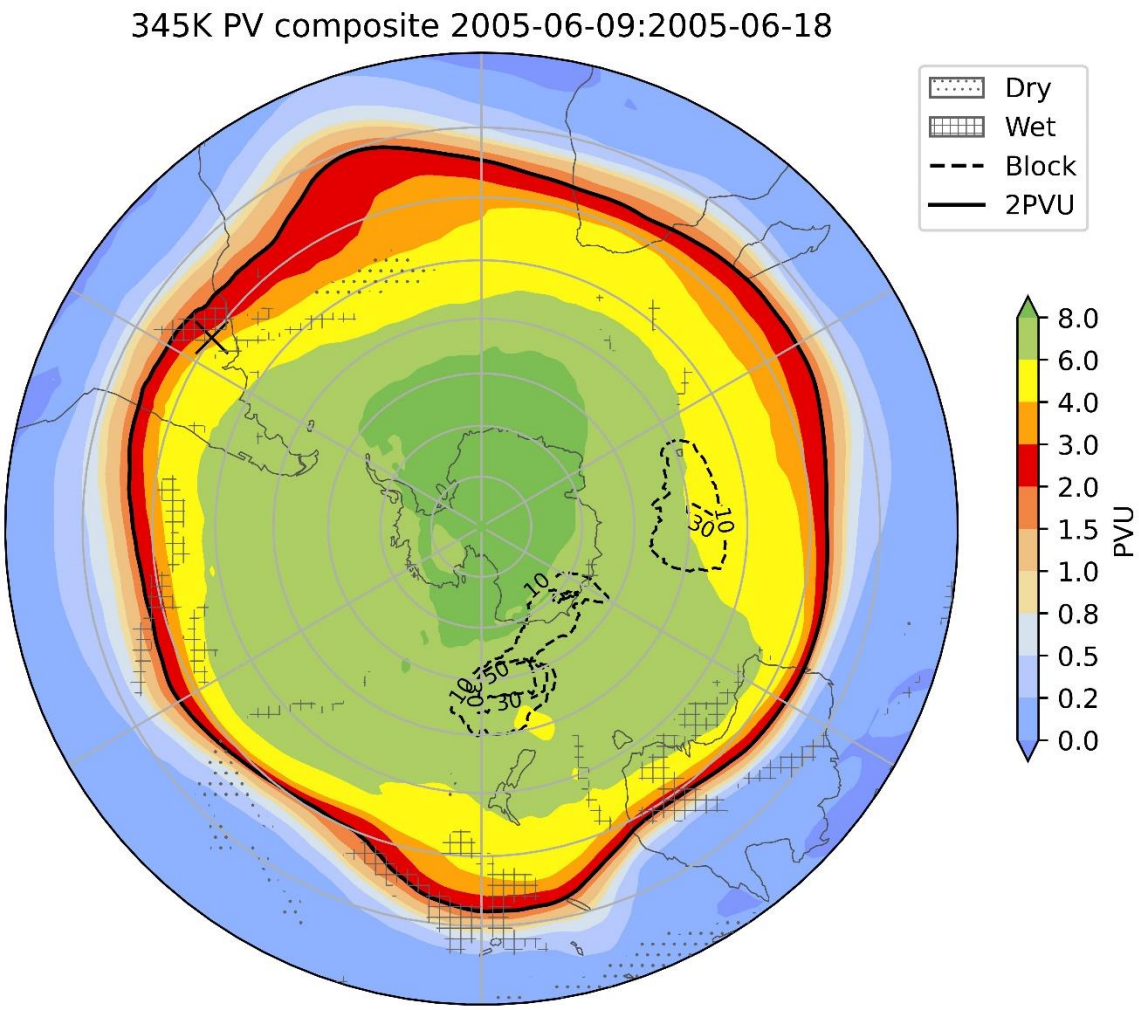

84

85 *S8. PV at 345 K isentrope averaged for the duration of the wet spell shown in S7 at the location "X".*
86 *Daily precipitation anomalies aggregated for the spell duration exceeding ±30 mm are indicated by*
87 *the corresponding hatches (see legend). Dashed contours show blocking frequency in % during this*
88 *period.*